

Semiexclusive production of vector mesons in proton-proton collisions with electromagnetic dissociation

Anna Cisek,^{1,*} Wolfgang Schäfer,^{2,†} and Antoni Szczurek^{2,1,‡}

¹*College of Natural Sciences, Institute of Physics,
University of Rzeszów, ul. Pigonia 1, PL-35-310 Rzeszów, Poland*

²*Institute of Nuclear Physics, Polish Academy of Sciences,
ul. Radzikowskiego 152, PL-31-342 Kraków, Poland*

Abstract

We calculate distributions of different vector mesons in purely exclusive ($pp \rightarrow ppV$) and semi-exclusive ($pp \rightarrow pXV$) processes with electromagnetic dissociation of a proton. The cross section for the electromagnetic dissociation is expressed through electromagnetic structure functions of the proton. We include the transverse momentum distribution of initial photons in the associated flux. Contributions of the exclusive and semi-exclusive processes are compared for different vector mesons ($V = \phi, J/\psi, Y$). We discuss how the relative contribution of the semi-exclusive processes depends on the mass of the vector meson as well as on different kinematical variables of the vector meson (y, p_t). The ratio of semi-exclusive to exclusive contributions are shown and compared for different mesons in different variables.

PACS numbers: 13.87.Ce, 14.65.Dw

*Electronic address: acisek@ur.edu.pl

†Electronic address: Wolfgang.Schafer@ifj.edu.pl

‡Electronic address: Antoni.Szczurek@ifj.edu.pl

I. INTRODUCTION

Exclusive production of vector mesons $pp \rightarrow ppV$ is a source of knowledge about gluon distributions in the proton. In contrast to the collinear approach, in the k_t -factorization approach the cross section depends not only on (unintegrated) gluon distribution function (UGDF) but also on the quarkonium quark-antiquark wave function [1]. It was shown that different UGDFs give different results. In order to “extract” or check the collinear gluon distribution or UGDF one has to be sure that the measured cross sections are not contaminated by any other mechanism.

So far both J/ψ and Y [2, 3] were measured in proton-proton collisions. The measurements are not fully exclusive as so far the outgoing protons were not measured. To increase the exclusivity of the reaction a rapidity veto (no emission around rapidity of vector meson) is being imposed. How good is such an approach is not fully understood in our opinion. In our earlier paper on J/ψ production [4] we have developed a formalism how to calculate such processes with rapidity gaps, but including proton dissociation. To calculate electromagnetic dissociation, the method uses parametrizations of the proton structure functions which are used to derive an inelastic photon flux. We have shown in [4] that the semi-exclusive mechanism cannot be completely removed by the requirement of rapidity veto. To our surprise the electromagnetic dissociation seems the most important (the largest) in this context. Here we wish to show more systematic studies for production of different vector mesons and better understand the competition of the purely exclusive and the semiexclusive processes.

The semiexclusive production mechanisms are shown for illustration in Fig.1. Here, due to the quantum numbers of vector mesons, the dominant mechanism is photon-pomeron fusion. As shown in the figure the photon can be coupled to either one of the two protons.

In this work, we will calculate different differential distributions. Of special interest is the ratio of semi-exclusive to exclusive cross section. Such a ratio may be considered as a measure of “unwanted” contamination of exclusive processes when using the rapidity gap method. The predictions of cross section for the semiexclusive processes may be also valuable as it could be in principle measured.

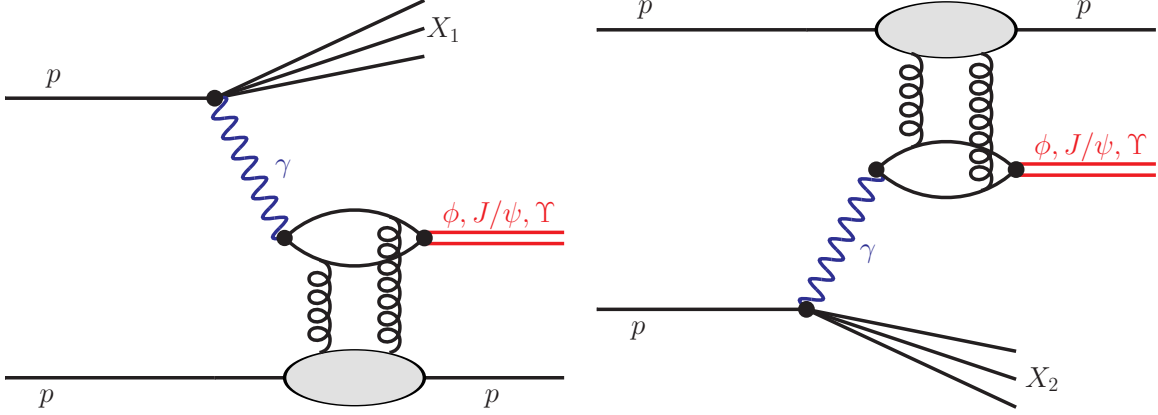


FIG. 1: Schematic representation of the electromagnetic excitation of one (left panel) or second (right panel) proton.

II. SKETCH OF THE FORMALISM

Let us concentrate on the events with electromagnetic dissociation of one of the protons. The important property of these processes is that the $p\gamma^* \rightarrow X$ transition is given by the electromagnetic structure functions of the proton, and thus to a large extent calculable “from data”. The cross section for such processes can be written as:

$$\frac{d\sigma(pp \rightarrow XVp; s)}{dyd^2\mathbf{p}dM_X^2} = \int \frac{d^2\mathbf{q}}{\pi\mathbf{q}^2} \mathcal{F}_{\gamma/p}^{(\text{inel})}(z_+, \mathbf{q}^2, M_X^2) \frac{1}{\pi} \frac{d\sigma^{\gamma^*p \rightarrow Vp}}{dt}(z_+, s, t = -(\mathbf{q} - \mathbf{p})^2) + (z_+ \leftrightarrow z_-), \quad (2.1)$$

where $z_{\pm} = e^{\pm y} \sqrt{(\mathbf{p}^2 + m_V^2)}/s$ is the fraction of the proton’s longitudinal momentum carried by the photon, and M_X is the invariant mass of the excited system X , \mathbf{p} is the transverse momentum of the vector meson, and $-\mathbf{q}$ is the transverse momentum of the outgoing hadronic system X . Below we also use $p_t = |\mathbf{p}|$ for the absolute value of the transverse momentum. The mass of the excited hadronic system must be above the threshold $M_{\text{thr}} = m_{\pi} + m_p$. In the kinematics of interest the “fully unintegrated” flux of photons associated with the breakup of the proton is calculable in terms of the structure function F_2 of a proton :

$$\mathcal{F}_{\gamma/p}^{(\text{inel})}(z, \mathbf{q}^2, M_X^2) = \frac{\alpha_{\text{em}}}{\pi} (1-z) \theta(M_X^2 - M_{\text{thr}}^2) \frac{F_2(x_{Bj}, Q^2)}{M_X^2 + Q^2 - m_p^2} \left[\frac{\mathbf{q}^2}{\mathbf{q}^2 + z(M_X^2 - m_p^2) + z^2 m_p^2} \right]^2, \quad (2.2)$$

where we calculate the photon virtuality Q^2 and the Bjorken variable x_{Bj} from

$$Q^2 = \frac{1}{1-z} \left[\mathbf{q}^2 + z(M_X^2 - m_p^2) + z^2 m_p^2 \right], \quad x_{Bj} = \frac{Q^2}{Q^2 + M_X^2 - m_p^2}. \quad (2.3)$$

We use the following parametrizations of the proton structure function $F_2(x, Q^2)$:

1. A parametrization of Ref. [5, 6] which is fitted to the lower energy CLAS data and is meant to give an accurate description especially in the resonance region $M_X \lesssim 2 \text{ GeV}$. In the figures it will be labeled as FFJLM. This parametrization does not describe data well, when it is extrapolated beyond the region of its intended use. Therefore we only use it when calculating observables with $M_X \lesssim 2 \text{ GeV}$.
2. The Abramowicz-Levy-Levin-Maor fit [7, 8] used previously also in [9], abbreviated here ALLM.
3. A newly constructed parametrization, which at $Q^2 > 9 \text{ GeV}^2$ uses an NNLO calculation of F_2 and F_L from NNLO MSTW 2008 partons [10]. It employs a useful code by the MSTW group [10] to calculate structure functions. At $Q^2 > 9 \text{ GeV}^2$ this fit uses the parametrization of Bosted and Christy [11] in the resonance region, and a version of the ALLM fit published by the HERMES Collaboration [12] for the continuum region. It also uses information on the longitudinal structure function from SLAC [13]. As the fit is constructed closely following the LUXqed work Ref.[14, 15], we call this fit LUX-like.
4. A Vector-Meson-Dominance model inspired fit of F_2 proposed in [16] at low Q^2 , which is completed by the same NNLO MSTW structure function as above at large Q^2 . This fit is labelled SU for brevity.

Our formalism is valid for photons which carry momentum fractions $z \ll 1$, this is an appropriate approximation for the production of vector mesons away from the forward rapidity regions. The differential cross section for the $\gamma^* p \rightarrow V p$ process is

$$\frac{d\sigma^{\gamma^* p \rightarrow V p}}{dt} = \frac{d\sigma_T^{\gamma^* p \rightarrow V p}}{dt} + \frac{d\sigma_L^{\gamma^* p \rightarrow V p}}{dt} = \frac{d\sigma_T^{\gamma^* p \rightarrow V p}}{dt} \left(1 + R_{LT}(Q^2) \right). \quad (2.4)$$

We parametrize the differential cross section by a simple analytic form as in Ref. [1] for J/Ψ . An analogous analysis was made in the papers [17, 18] and experimental data can

be found in [19, 20]. In Fig. 2 we show as an example the differential cross section for ϕ photoproduction, comparing our simple fit with the data taken by the ZEUS collaboration at HERA [21].

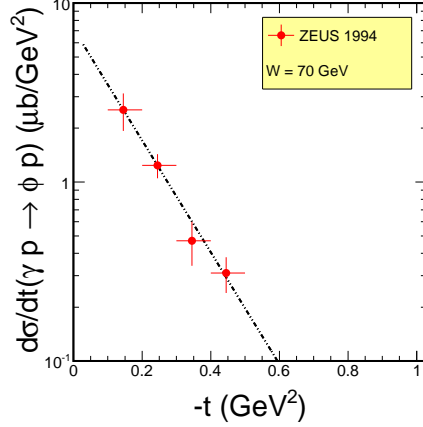


FIG. 2: Differential cross section for diffractive photoproduction of ϕ mesons. Data are from the ZEUS collaboration at HERA [21].

III. RESULTS

We start our discussion of results with the rapidity- and transverse-momentum distributions of semi-exclusively produced ϕ -mesons. Here we want to discuss the effect of longitudinal photons quantified by R_{LT} in Eq.(2.4). In Fig. 3 we show the rapidity dependent cross section

$$\frac{d\sigma(\phi)}{dy} \equiv \int_{M_{\text{thr}}}^{M_{X,\text{max}}} dM_X \frac{d\sigma(pp \rightarrow \phi X; s)}{dy dM_X}, \quad (3.1)$$

integrated up to masses $M_{X,\text{max}} = 10$ GeV with and without the R_{LT} -term included. We observe, that longitudinal photons enhance the cross section by about $\sim 20\%$ uniformly in y . As we can see from the transverse-momentum distribution of ϕ -mesons shown in Fig. 4, the effect of longitudinal photons is important at large transverse momenta, $p_t > 1$ GeV. For heavier mesons we find small effects of longitudinal photons, as the ratio behaves like $R_{LT} \propto Q^2/m_V^2$, over a broad range of Q^2 . This means a suppression of longitudinal photons in the relevant for us range of Q^2 .

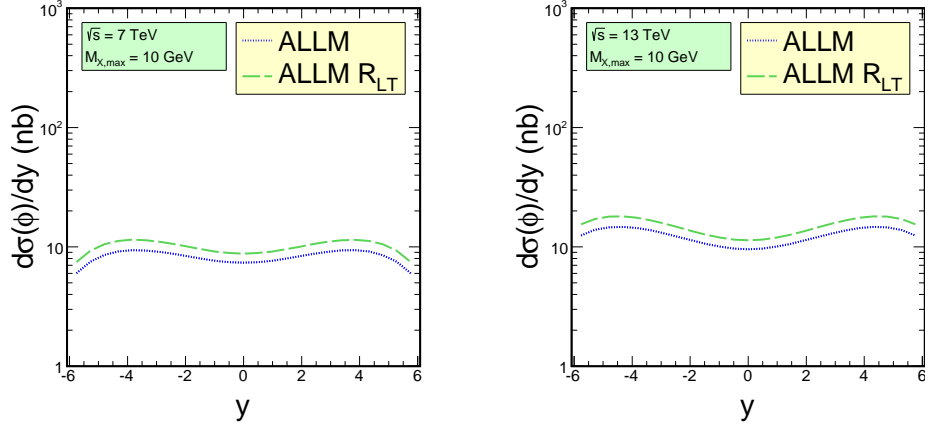


FIG. 3: Rapidity distribution of ϕ -mesons at two different energies, with and without the contribution from longitudinal photons.

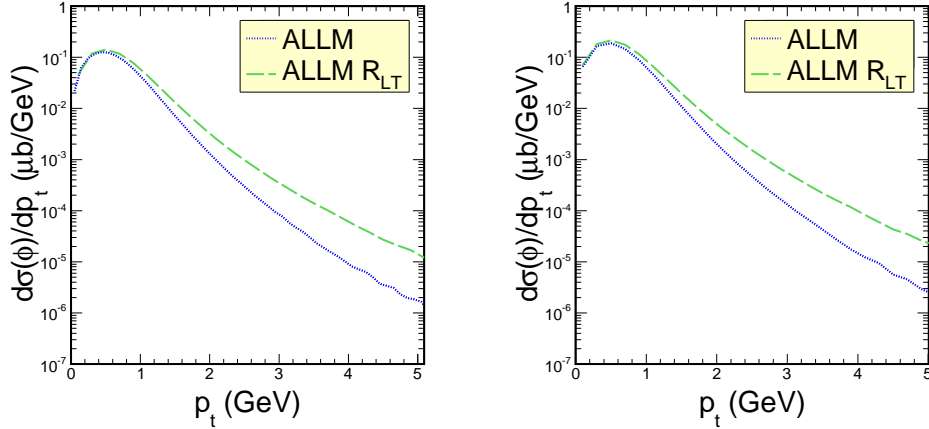


FIG. 4: Transverse momentum distribution of ϕ -mesons at two different energies, with and without the contribution from longitudinal photons for energy $\sqrt{s} = 7$ TeV (left panel) and $\sqrt{s} = 13$ TeV (right panel).

We now wish to present results for rapidity and transverse-momentum distributions of mesons. In Figs. 5 and 6 we show the rapidity dependent cross section

$$\frac{d\sigma(V)}{dy} \equiv \int_{M_{\text{thr}}}^{M_{X,\text{max}}} dM_X \frac{d\sigma(pp \rightarrow VX; s)}{dy dM_X}, \quad (3.2)$$

for $V = \phi, J/\psi, Y$ and $M_{X,\text{max}} = 10$ GeV, using different parametrizations of the proton structure function F_2 . We observe a good agreement of the results obtained with different

parametrizations. The rapidity distributions become narrower the heavier the produced meson. In Figs. 7 and 8 we show the distributions in transverse momentum squared of the meson. Again we integrate up to $M_{X,\max} = 10 \text{ GeV}$:

$$\frac{d\sigma(V)}{dp_t^2} \equiv \int_{M_{\text{thr}}}^{M_{X,\max}} dM_X \frac{d\sigma(pp \rightarrow VX; s)}{dp_t^2 dM_X}. \quad (3.3)$$

Also the transverse momentum distributions show a good agreement for the different parametrizations of the proton structure function. We see that up to $p_t^2 \lesssim 2 \text{ GeV}^2$ the p_t^2 -distributions have an approximate exponential behaviour $\propto \exp[-B_{\text{inel}} p_t^2]$.

In Fig. 9 we show the distribution in the invariant mass M_X of the excited system. Here we see, that the Fiore-fit behaves very differently from the other parametrizations at $M_X > 2 \text{ GeV}$. Due to this unphysical behaviour, it cannot be used for large M_X . On the other hand, the Szczurek-Uleshchenko parametrization appears to underestimate the cross section in the resonance region of small M_X . Here the LUX-type fit, ALLM and the Fiore parametrizations agree quite well.

Let us have a closer look at the correlation of the M_X -dependence with rapidity of the vector meson. In Fig. 10 we show the rapidity distribution of mesons for ALLM structure function of proton and different bins of $M_X \in [M_{X,\min}, M_{X,\max}]$. We observe that rapidity distributions for bins with $M_X > 10 \text{ GeV}$ are peaked at midrapidity and are somewhat narrower than the contribution of $M_X \leq 10 \text{ GeV}$.

In Fig. 11 we show the rapidity distribution of mesons for different bins of M_X for FFJLM structure function of proton, similarly as Fig. 10.

We return to the transverse momentum distributions in Fig. 12, where we plot the p_t^2 -distribution with M_X integrated up to different values of $M_{x,\max}$. We observe that the contribution from the resonance region of $M_X < 2 \text{ GeV}$ has a much softer tail at large p_t^2 than when the large-mass contribution is added. For comparison, we also show the p_t^2 -distribution of the exclusive $pp \rightarrow ppV$ contribution [1]. The theoretical analysis for exclusive photoproduction in proton-proton collisions was shown also in papers [22–24]. The shape of the p_t^2 -distributions only weakly depends on energy.

Under the conditions of LHC experiments, like [2, 3], the dissociative diffractive production is a background to the fully exclusive production with intact protons.

In order to highlight the difference of the inelastic contribution and the exclusive one,

we introduce the ratios:

$$R^{\text{EM/excl.}}(p_t, M_{X,\text{max}}) = \frac{\int_{M_{\text{thr}}}^{M_{X,\text{max}}} dM_X \frac{d\sigma(pp \rightarrow pVX)}{dp_t dM_X}}{\frac{d\sigma(pp \rightarrow pVp)}{dp_t}},$$

$$R^{\text{EM/excl.}}(y, M_{X,\text{max}}) = \frac{\int_{M_{\text{thr}}}^{M_{X,\text{max}}} dM_X \frac{d\sigma(pp \rightarrow pVX)}{ydM_X}}{\frac{d\sigma(pp \rightarrow pVp)}{dy}}. \quad (3.4)$$

In Fig. 13 we show the ratio $R^{\text{EM/excl.}}$ as a function of p_t for different upper limits on M_X , we see that as soon high mass states are included, the inelastic contribution dominates at $p_t \gtrsim 1$ GeV. In Fig. 14 we have a closer look at $R^{\text{EM/excl.}}$ for the excitation of low-mass states $M_X < 2$ GeV. Here we use both the ALLM and Fiore parametrizations. We see that for ϕ production the ratio is always smaller than one, while for heavier mesons, inelastic production will dominate at $p_t \gtrsim 1.5$ GeV.

In Figs. 15 and 16 we show the analogous ratios for the rapidity distribution.

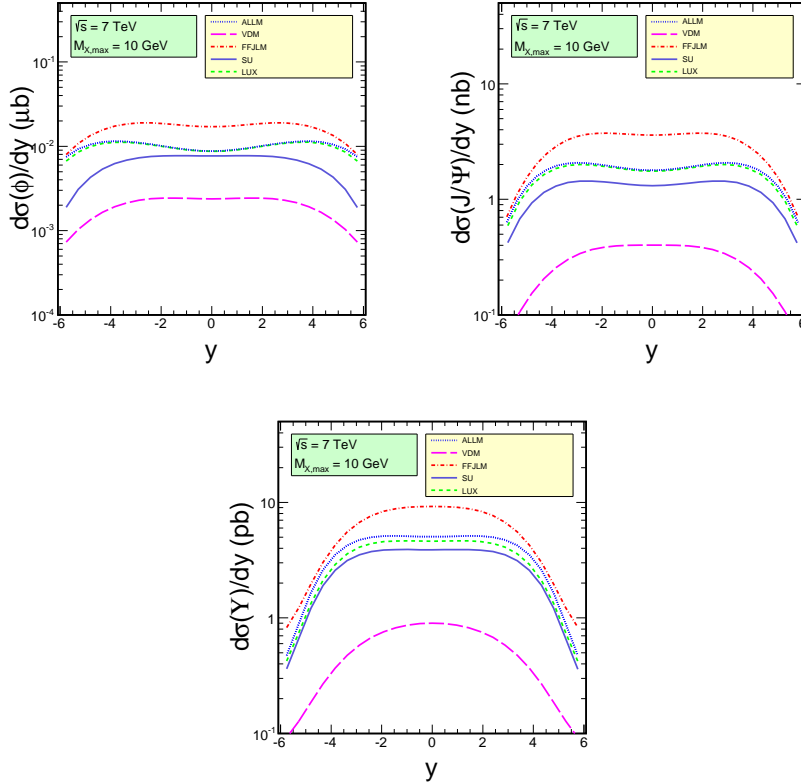


FIG. 5: Rapidity distribution for pp cm-energy $\sqrt{s} = 7$ TeV for the production of ϕ , J/ψ and Y mesons for different parametrizations of the proton structure function F_2 .

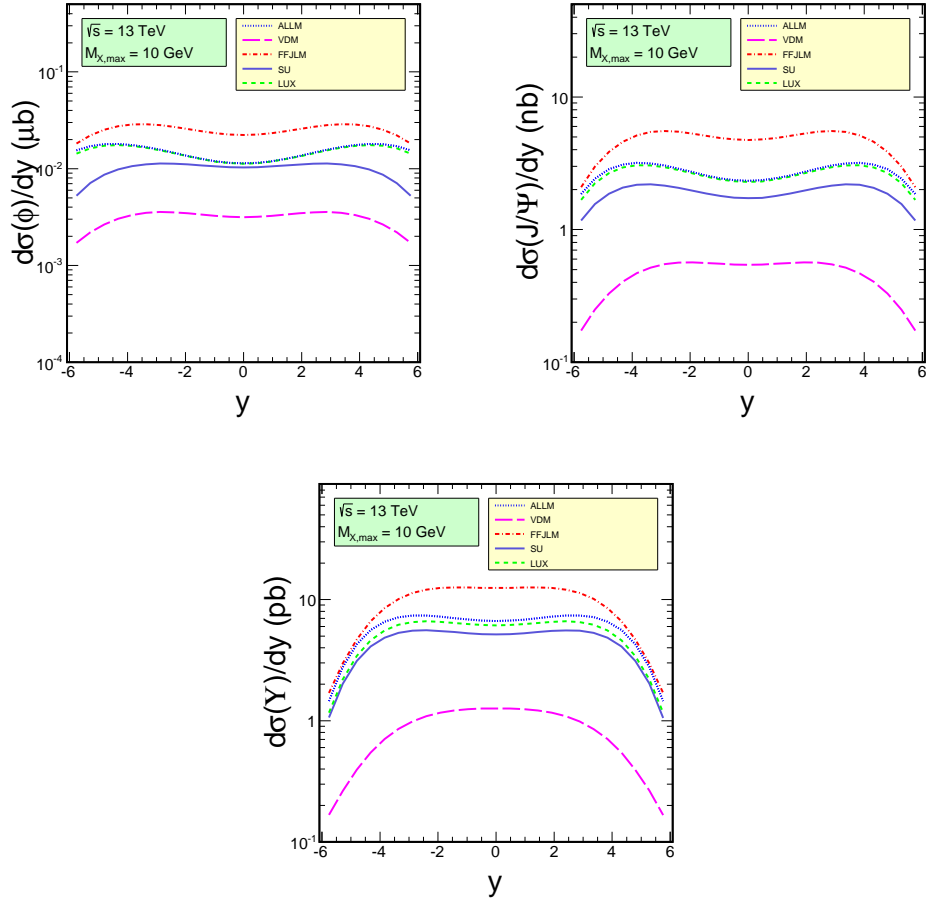


FIG. 6: Rapidity distribution for pp cm-energy $\sqrt{s} = 13$ TeV for the production of $\phi, J/\psi$ and Y mesons for different parametrizations of the proton structure function F_2 .

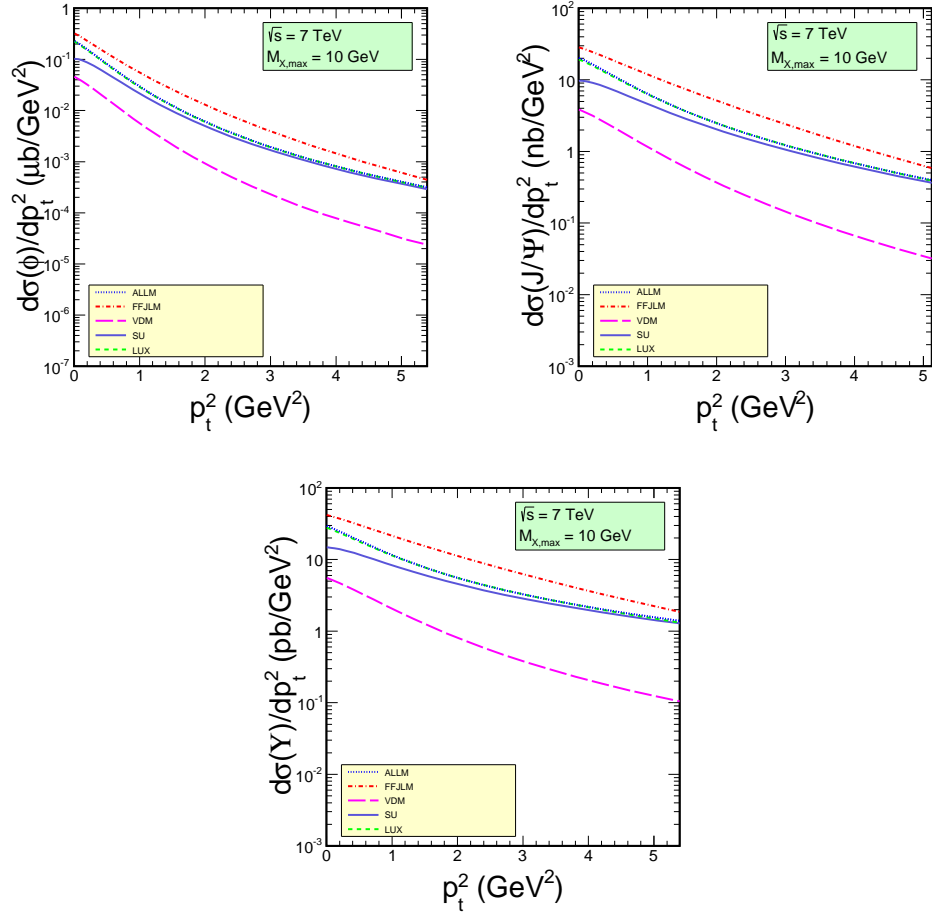


FIG. 7: Transverse momentum distribution of vector meson for pp cm-energy $\sqrt{s} = 7$ TeV for the production of ϕ , J/ψ and Y mesons for different parametrizations of the proton structure function F_2 .

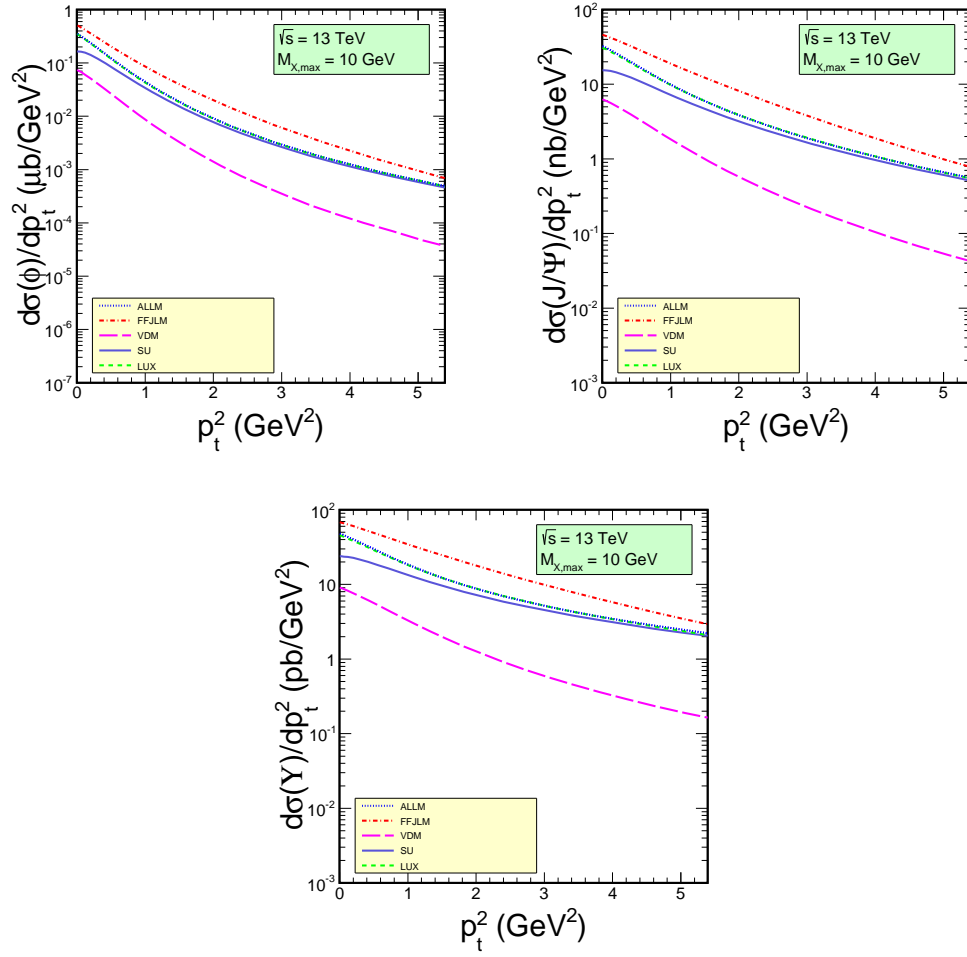


FIG. 8: Transverse momentum distribution of vector meson for pp cm-energy $\sqrt{s} = 13$ TeV for the production of ϕ , J/ψ and Y mesons for different parametrizations of the proton structure function F_2 .

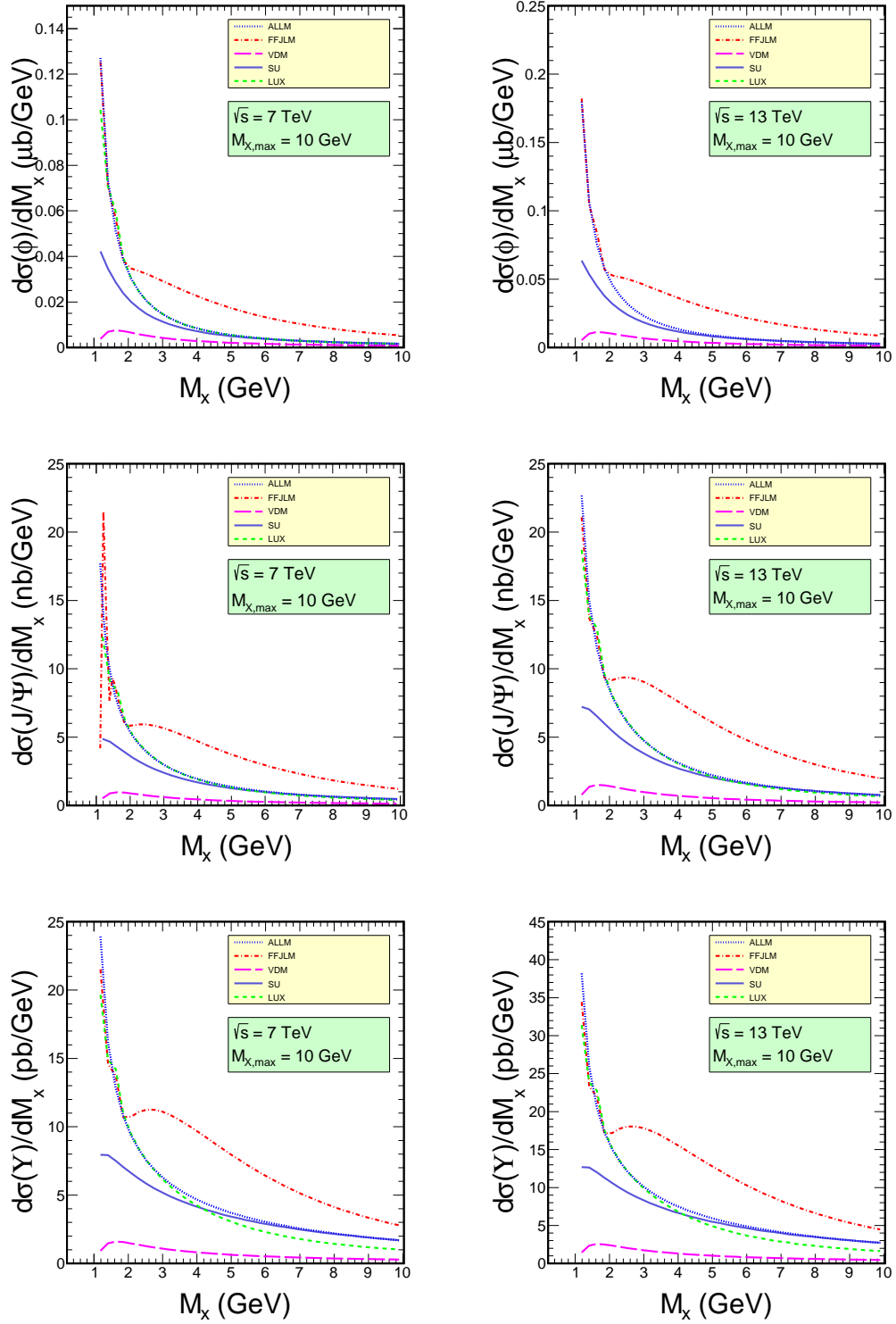


FIG. 9: Distribution of the invariant mass M_X of the excited system for the pp cm-energy $\sqrt{s} = 7$ TeV (left panels) and $\sqrt{s} = 13$ TeV (right panels).

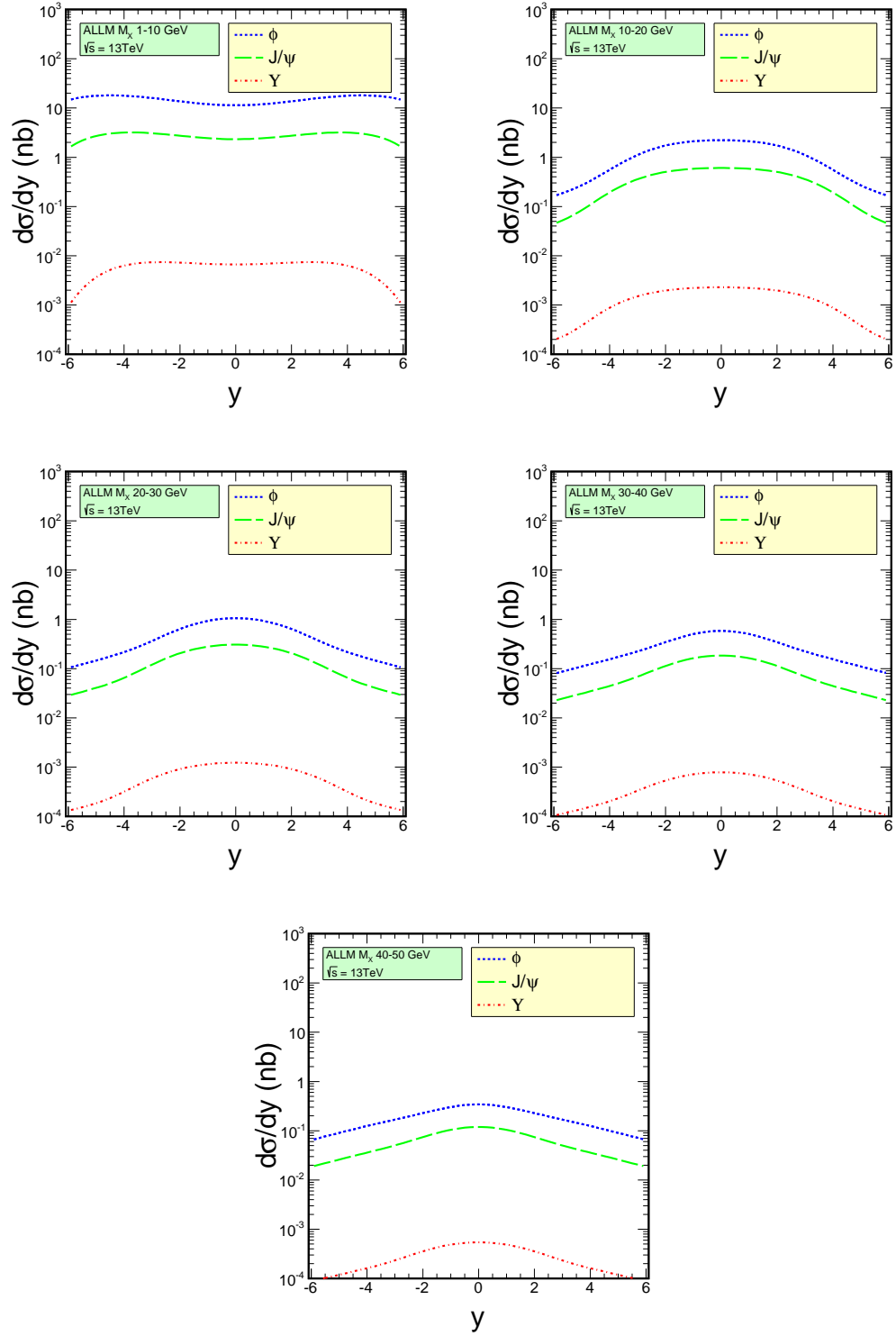


FIG. 10: Rapidity distribution of vector mesons for different bins of the invariant mass of the excited system for the ALLM parametrisation.

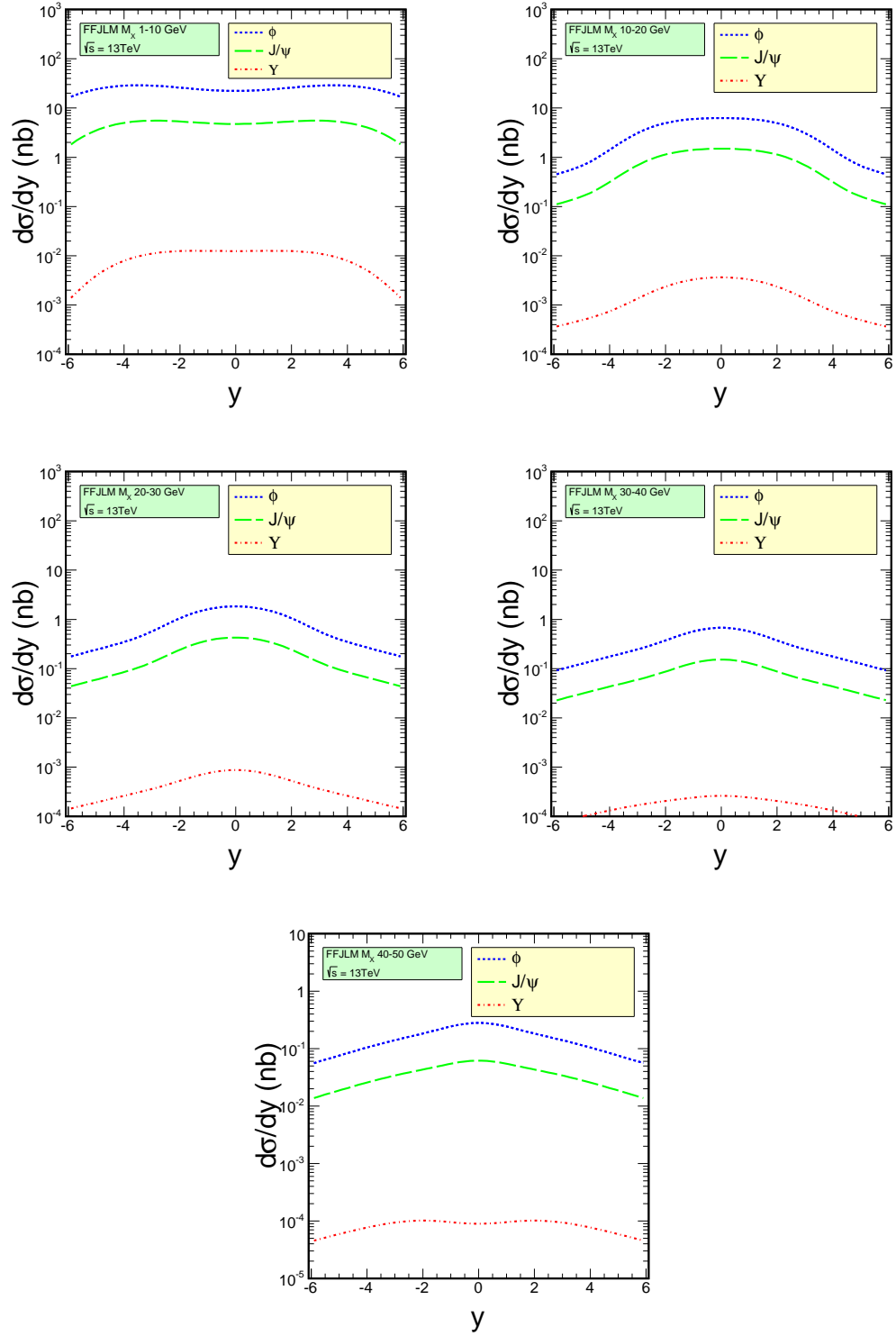


FIG. 11: Rapidity distribution of vector mesons for different bins of the invariant mass of the excited system for the FFJLM parametrization.

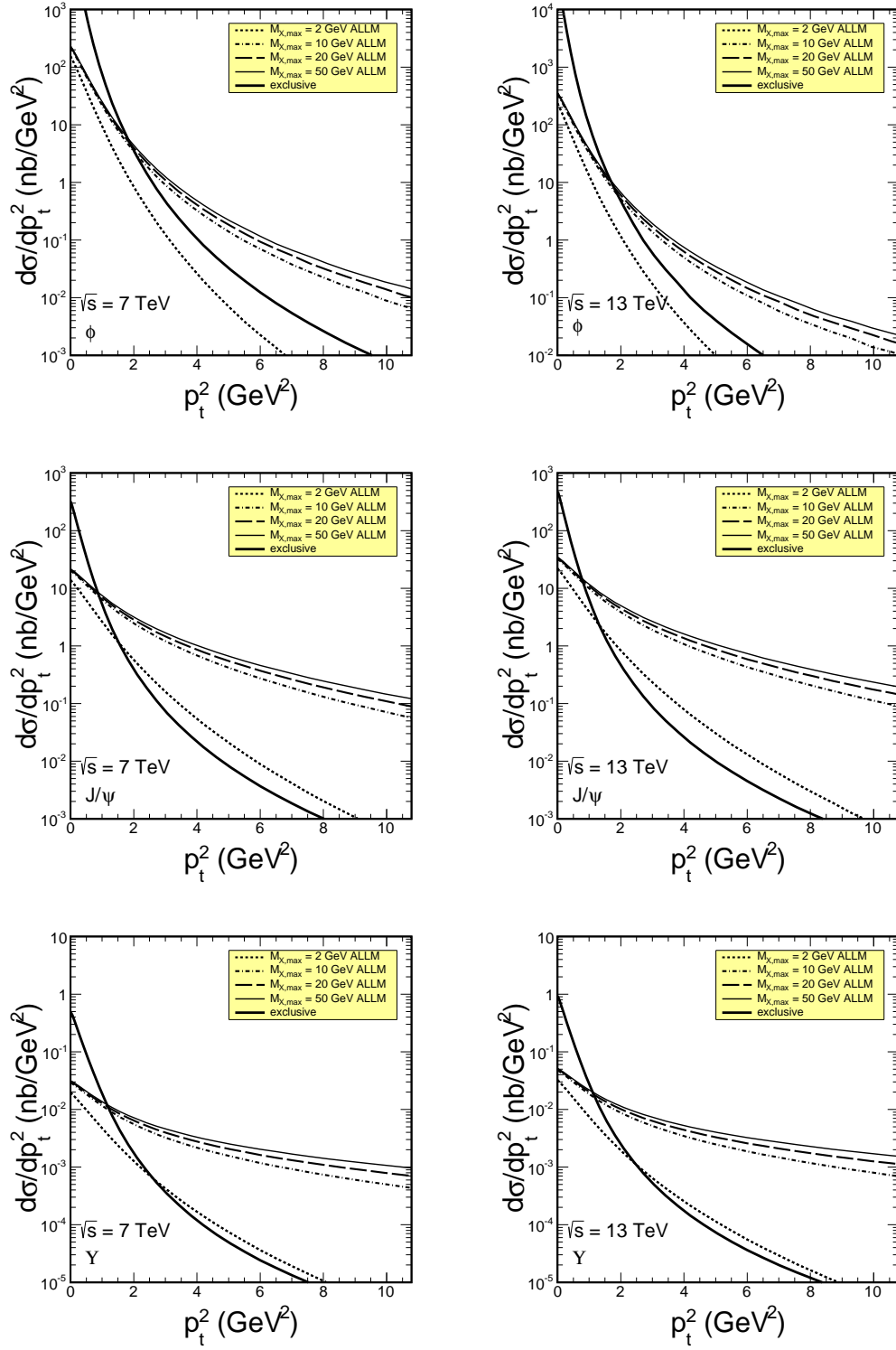


FIG. 12: p_t^2 -distribution of vector mesons for different upper limits on the invariant mass of the excited system.

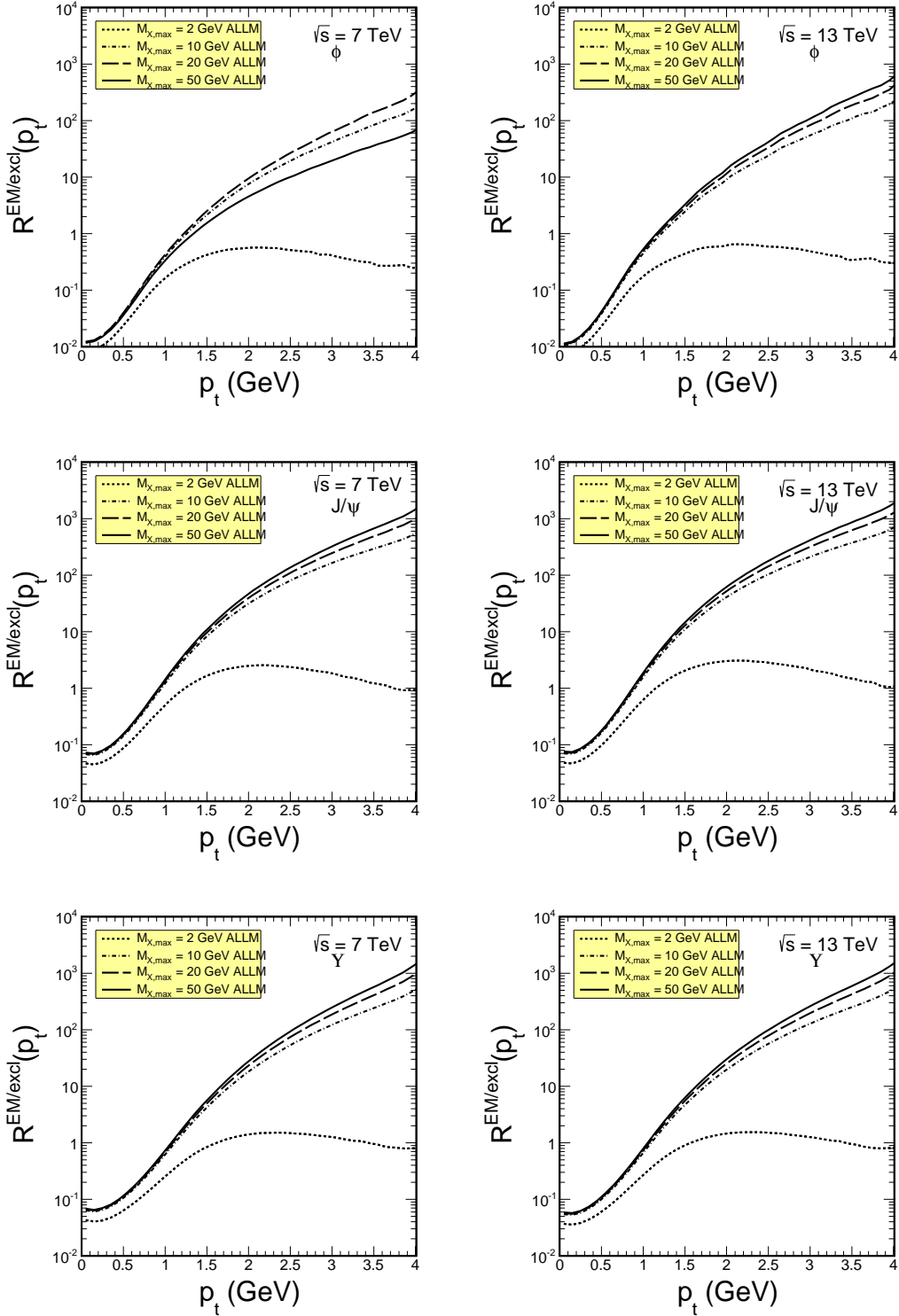


FIG. 13: Ratio of inelastic diffractive to exclusive vector meson production as a function of transverse momentum for different upper limits on the excited mass M_X .

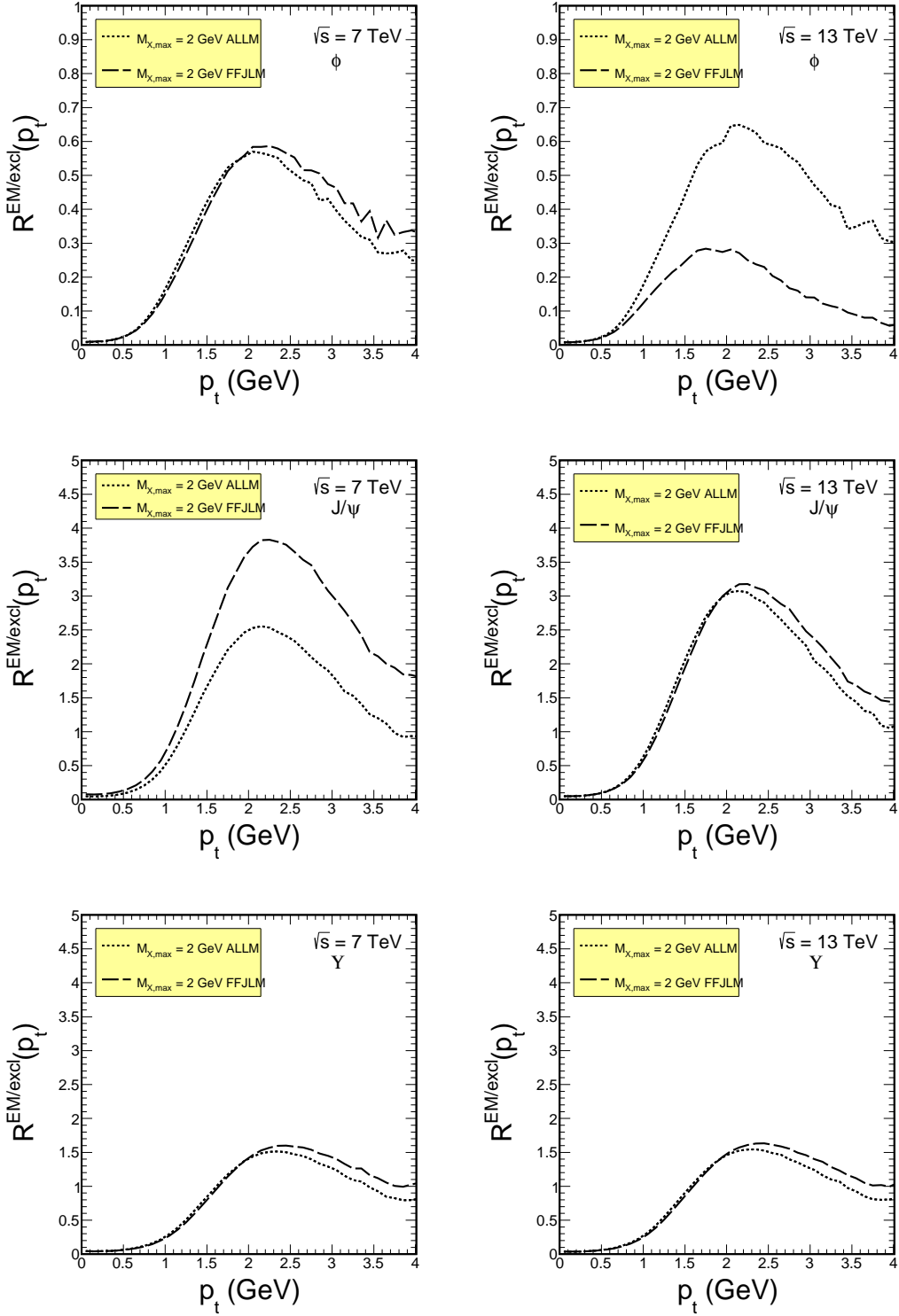


FIG. 14: Ratio of inelastic diffractive to exclusive vector meson production as a function of transverse momentum for low proton excited masses, integrated up to $M_X = 2$ GeV.

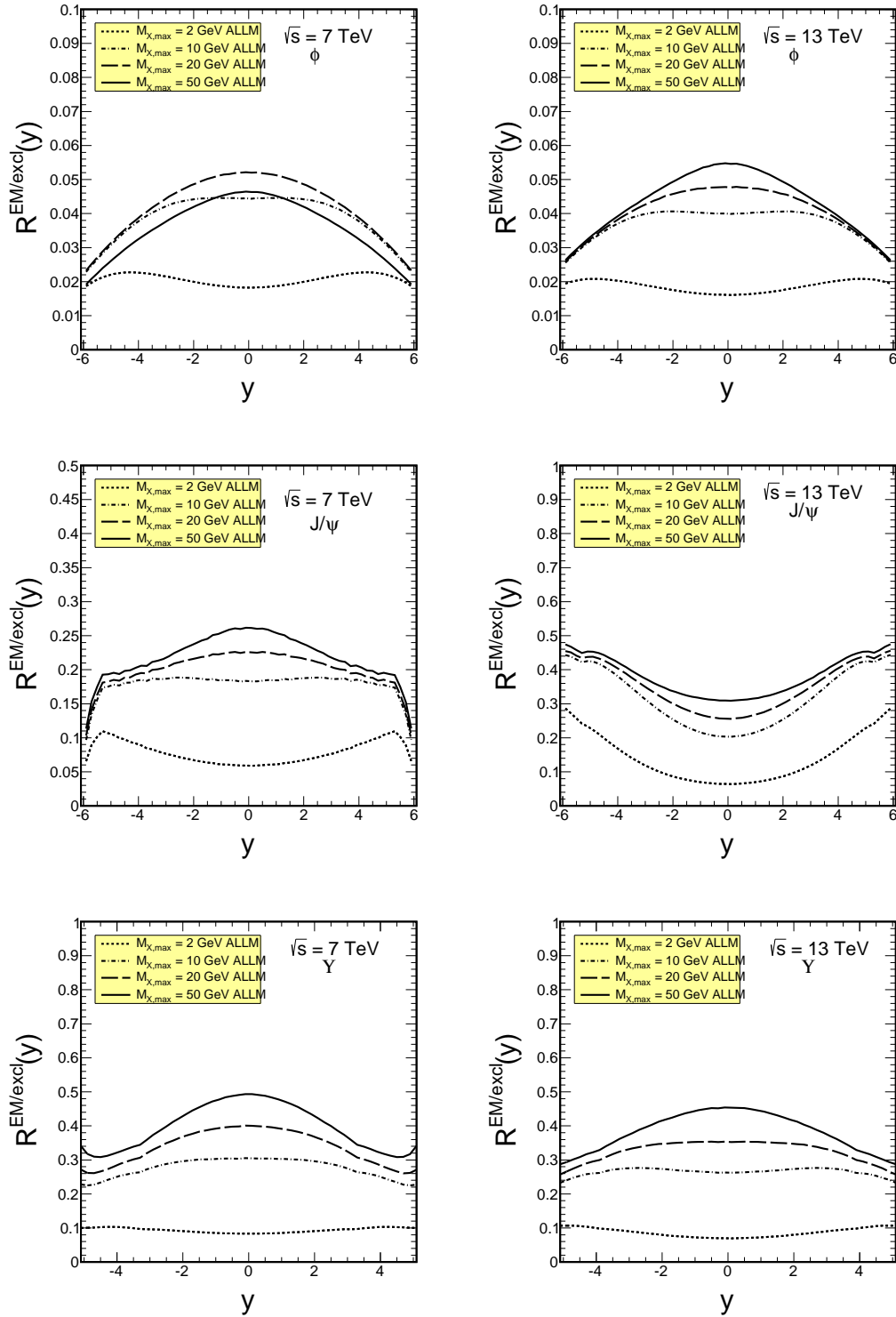


FIG. 15: Ratio of inelastic diffractive to exclusive vector meson production as a function of rapidity for different upper limits on the excited mass M_X .

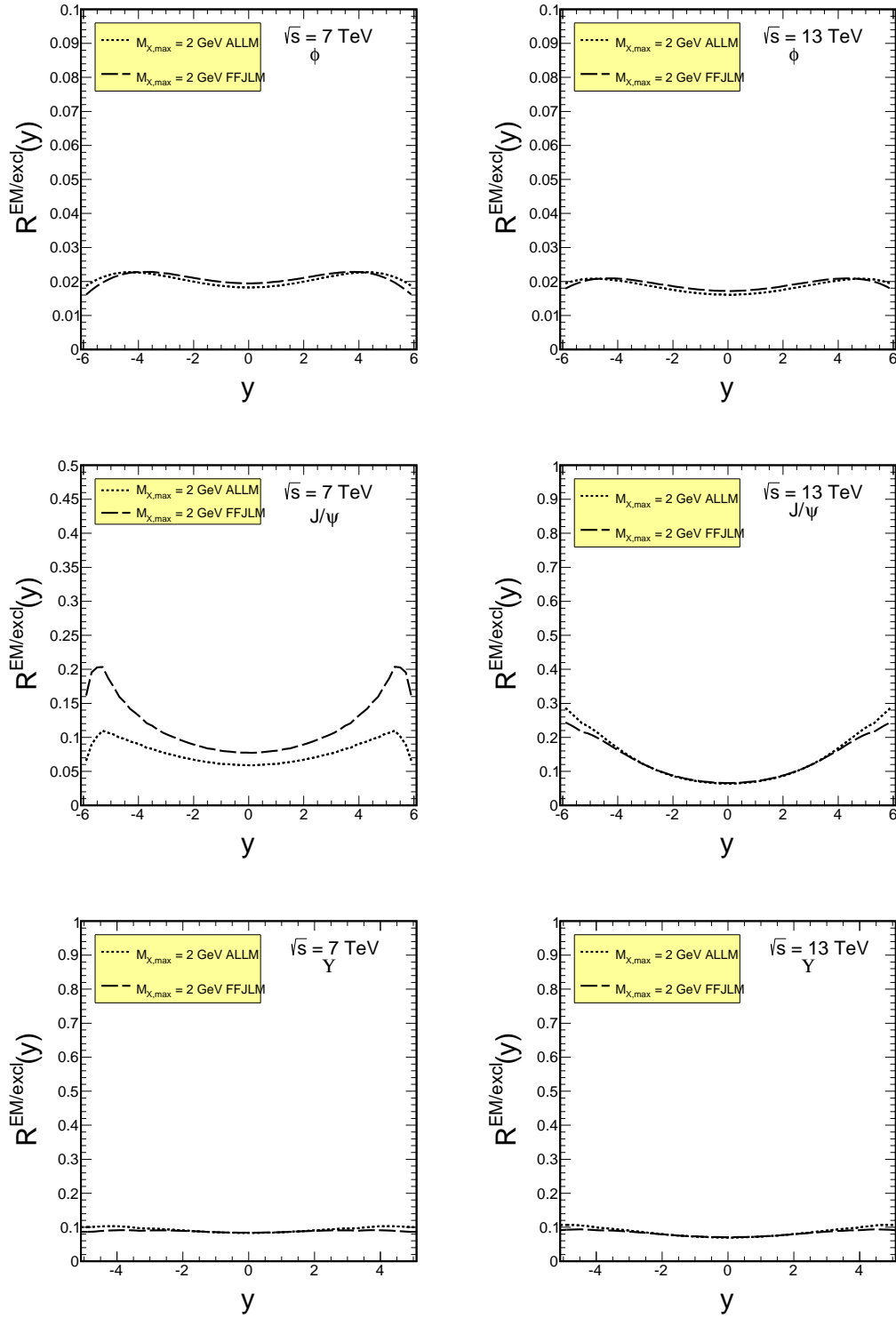


FIG. 16: Ratio of inelastic diffractive to exclusive vector meson production as a function of rapidity for low excited masses, integrated up to $M_X = 2$ GeV.

IV. CONCLUSIONS

In this paper we have discussed semiexclusive production of vector mesons in $pp \rightarrow VpX$ processes via photon-pomeron or pomeron-proton fusion, where X stands for excited/dissociated proton system and $V = \phi, J/\psi, Y$. We have investigated the similarities and differences of various cross sections to the exclusive $pp \rightarrow ppV$ process. Electromagnetic dissociation of protons is calculated using an inelastic unintegrated photon flux which was calculated based on modern parametrizations of deep-inelastic proton structure functions. Different parametrizations from the literature have been used.

A number of differential cross distributions for the vector mesons (in their rapidity and transverse momentum) as well as for the mass of the dissociative system, remnant of the proton, have been calculated. We have found that in all the considered cases the photon dissociation cross section is large compared to its purely exclusive counterpart. The results strongly depend on the parametrization of the structure function used. One should stress, however, in this context that different parametrizations have quite different status. Some of them are global fits to the world data, often not ideal in some other regions of the phase space. Some of them focus rather on some corners of the phase space, so are extremely good there. However, they can be not realistic in other corners of the phase space. We have discussed in detail which distributions provide realistic estimates of the cross section.

The semiexclusive contributions produce vector mesons with large transverse momenta. The rapidity distributions of semi-exclusive and purely exclusive distributions are rather similar. In the present analysis we have shown also the ratio of the semiexclusive to the purely exclusive contributions. This ratio depends strongly on the vector meson transverse momentum and only mildly on rapidity. In general, a bigger ratio is obtained for heavier quarkonia.

It is obvious that a large fraction of the remnant cannot be seen by central detectors of different LHC experiments in the case when protons are not measured using specially dedicated forward detectors, just installed recently by the CMS-TOTEM or ATLAS collaborations. Without measuring both protons, as is the case of the LHCb experiment, the so-called exclusive data are not fully exclusive and may contain the semi-exclusive contributions discussed here. The LHCb collaboration cuts the large- p_t part of the correspond-

ing distribution in a purely phenomenological fit of different slope. It is not completely clear how good is such a procedure. It would be good to relax requirements on rapidity gap(s) around vector mesons and actually measure the semieexclusive contributions. We encourage experimentalists to perform such analyses. We note that the semiexclusive contributions were not measure so far, but are interesting themselves. Such measurements would be therefore tests of the method used here.

Acknowledgments

This work was partially supported by the Polish National Science Center grant UMO-2018/31BST2/03537 and by the Centre for Innovation and Transfer of Natural Sciences and Engineering Knowledge in Rzeszów.

-
- [1] A. Cisek, W. Schäfer and A. Szczurek, JHEP **1504** (2015) 159.
 - [2] R. Aaij *et al.* [LHCb Collaboration], J. Phys. G **40** (2013) 045001 [arXiv:1301.7084 [hep-ex]].
 - [3] R. Aaij *et al.* [LHCb Collaboration], JHEP **1509** (2015) 084 [arXiv:1505.08139 [hep-ex]].
 - [4] A. Cisek, W. Schäfer and A. Szczurek, Phys. Lett. B **769**, 176 (2017) [arXiv:1611.08210 [hep-ph]].
 - [5] R. Fiore, A. Flachi, L. L. Jenkovszky, A. I. Lengyel and V. K. Magas, Eur. Phys. J. A **15** (2002) 505 [hep-ph/0206027].
 - [6] R. Fiore, L. L. Jenkovszky, F. Paccanoni and A. Prokudin, Phys. Rev. D **70**, 054003 (2004) [hep-ph/0404021].
 - [7] H. Abramowicz, E. M. Levin, A. Levy and U. Maor, Phys. Lett. B **269** (1991) 465.
 - [8] H. Abramowicz and A. Levy, hep-ph/9712415.
 - [9] M. Łuszczak, W. Schäfer and A. Szczurek, Phys. Rev. D **93**, no. 7, 074018 (2016) [arXiv:1510.00294 [hep-ph]].
 - [10] A. D. Martin, W. J. Stirling, R. S. Thorne and G. Watt, Eur. Phys. J. C **63**, 189 (2009) [arXiv:0901.0002 [hep-ph]].
 - [11] P. E. Bosted and M. E. Christy, Phys. Rev. C **77**, 065206 (2008) [arXiv:0711.0159 [hep-ph]].
 - [12] A. Airapetian *et al.* [HERMES Collaboration], JHEP **1105**, 126 (2011) [arXiv:1103.5704 [hep-ex]].
 - [13] K. Abe *et al.* [E143 Collaboration], Phys. Lett. B **452**, 194 (1999) doi:10.1016/S0370-

- 2693(99)00244-0 [hep-ex/9808028].
- [14] A. Manohar, P. Nason, G. P. Salam and G. Zanderighi, Phys. Rev. Lett. **117** (2016) no.24, 242002 [arXiv:1607.04266 [hep-ph]].
- [15] A. V. Manohar, P. Nason, G. P. Salam and G. Zanderighi, JHEP **1712** (2017) 046 [arXiv:1708.01256 [hep-ph]].
- [16] A. Szczurek and V. Uleshchenko, Eur. Phys. **C12** (2000) 663; Phys. Lett. **B475** (2000) 120.
- [17] I. P. Ivanov, N. N. Nikolaev and A. A. Savin, Phys. Part. Nucl. **37** (2006) 1 [hep-ph/0501034].
- [18] W. Schäfer and A. Szczurek, Phys. Rev. **D76** (2007) 094014.
- [19] C. Alexa *et al.* [H1 Collaboration], Eur. Phys. J. C **73**, no. 6, 2466 (2013) [arXiv:1304.5162 [hep-ex]].
- [20] A. Aktas *et al.* [H1 Collaboration], Phys. Lett. B **568**, 205 (2003) [hep-ex/0306013].
- [21] M. Derrick *et al.* [ZEUS Collaboration], Phys. Lett. B **377** (1996) 259-272 [arXiv:9601009 [hep-ex]].
- [22] L. Motyka and G. Watt, Phys. Rev. D **78**, 014023 (2008) [arXiv:0805.2113 [hep-ph]].
- [23] S. P. Jones, A. D. Martin, M. G. Ryskin and T. Teubner, JHEP **1311**, 085 (2013) [arXiv:1307.7099 [hep-ph]].
- [24] V. P. Goncalves, L. A. S. Martins and W. K. Sauter, Eur. Phys. J. C **76**, no. 2, 97 (2016) [arXiv:1511.00494 [hep-ph]].